European Journal of Immunology

Influenza and dengue virus co-infection impairs monocyte recruitment to the lung, increases dengue virus titers, and exacerbates pneumonia

Michael A. Schmid[1], Karla N. González[1,2], Sanjana Shah[1], José Peña[3], Matthias Mack[4], Laura B. Talarico[5], Fernando P. Polack[5], and Eva Harris[1]**

[1] Division of Infectious Diseases and Vaccinology, School of Public Health, University of California, Berkeley, Berkeley, California, USA

[2] Laboratorio Nacional de Virología, Centro Nacional de Diagnóstico y Referencia, Ministerio de Salud, Managua, Nicaragua

[3] Lawrence Livermore National Laboratory, Livermore, California, USA

[4] Department of Internal Medicine, University Hospital Regensburg, Regensburg, Germany

[5] Fundación INFANT, Buenos Aires, Argentina

*Co-corresponding authors: michael.alex.schmid@gmail.com (MAS) and

eharris@berkeley.edu (EH) for communication with the Editorial and Production offices

Division of Infectious Diseases and Vaccinology, School of Public Health, University of California, Berkeley, 185 Li Ka Shing Center, 1951 Oxford Street, Berkeley, CA 94720-3370, USA

Tel. +1 510 642-4845, Fax +1 510 642-6350

Received: 12-Aug-2016; Revised: 19-Nov-2016; Accepted: 16-Dec-2016

This article has been accepted for publication and undergone full peer review but has not been through the copyediting, typesetting, pagination and proofreading process, which may lead to differences between this version and the Version of Record. Please cite this article as doi: 10.1002/eji.201646675.

List of abbreviations: DC, dendritic cell; DENV, dengue virus; EID_{50}, egg infectious dose-50; IFN, interferon; n.s., non-significant; PFU, plaque forming units; WT, wild type

Key words: influenza and dengue virus co-infection, immune response, monocyte, lung, pneumonia, pathogenesis

Abstract

Co-infections of influenza virus and bacteria are known to cause severe disease, but little information exists on co-infections with other acute viruses. Seasonal influenza and dengue viruses (DENV) regularly co-circulate in tropical regions. The pandemic spread of influenza virus H1N1 (hereafter H1N1) in 2009 led to additional severe disease cases that were co-infected with DENV. Here, we investigated the impact of co-infection on immune responses and pathogenesis in a new mouse model. Co-infection of otherwise sublethal doses of a Nicaraguan clinical H1N1 isolate and two days later with a virulent DENV2 strain increased systemic DENV titers and caused 90% lethality. Lungs of co-infected mice carried both viruses, developed severe pneumonia, and expressed a unique pattern of host mRNAs, resembling only partial responses against infection with either virus alone. A large number of monocytes were recruited to DENV-infected but not to co-infected lungs, and depletion and adoptive transfer experiments revealed a beneficial role of monocytes. Our study shows that co-infection with influenza and DENV impairs host responses, which fail to control DENV titers and instead, induce severe lung damage. Further, our findings identify key inflammatory pathways and monocyte function as targets for future therapies that may limit immunopathology in co-infected patients.

Graph Abstract

Single infection with pandemic influenza (H1N1) or dengue virus (DENV) induces mild airway inflammation and mild disease. In contrast, co-infected mice (H1N1–DENV) develop lethal disease that is characterized by lack of monocyte recruitment to the lung, truncated immune responses, severe pneumonia, and systemically increased dengue virus titers.

Introduction

Infections with influenza or dengue virus impose large global health and economic burdens. Clinical observations suggest that co-infection with influenza and dengue viruses may further increase disease severity [1-4].

Seasonal influenza viruses cause 3-5 million severe cases and 250,000-500,000 influenza-related deaths annually [5]. Influenza A virus is a member of the *Orthomyxoviridae* family, with a segmented (–)-sense RNA genome, and is classified in subtypes according to hemagglutinin (H) and neuraminidase (N) proteins [6]. After airborne transmission, influenza A virus infects epithelial cells of the respiratory tract [7] and causes respiratory disease, characterized by sudden onset of high fever, cough, headache, muscle pain, and severe malaise [5]. Reassortment of influenza virus gene segments from human, avian, and swine origins can generate new strains that cause global pandemics. The pandemic influenza A virus H1N1 that emerged globally in 2009 spread rapidly and caused 152,000-575,000 deaths within the first year [8].

Dengue is the most prevalent arthropod-borne viral disease in humans, with up to 390 million infections and 96 million dengue cases annually [9]. The four serotypes of dengue virus (DENV1-4) have a (+)-sense RNA genome and are members of the *Flaviviridae* family. After transmission via infected *Aedes* mosquitoes, DENV infects dendritic cells (DCs), macrophages, and *de novo*-recruited monocytes in the dermis [10, 11] and then spreads systemically [12, 13]. Dengue is characterized by high fever, muscle pain, and headache, and can progress to severe dengue, characterized by systemic vascular leak, hemorrhage, and/or circulatory shock [14]. While primary DENV infections usually cause uncomplicated dengue or subclinical disease, increased disease severity can occur during subsequent infection with a different serotype [15]. Serotype cross-reactive antibodies then enhance infection of monocytes and macrophages [16, 17] or memory T cells induce immunopathology [18].

Co-infections of influenza or DENV with other pathogens commonly occur. For DENV, co-infections with *Plasmodium* [19], chikungunya virus [20] or Zika virus [21] have been reported, and 1-7% of dengue patients had bacterial co-infections [22]. During influenza A virus infection, opportunistic bacteria cause most influenza-related deaths [23]. Little information, however, exists regarding whether co-infection of influenza with other acute viruses affect disease outcome. Seasonal influenza A virus and DENV epidemics regularly overlap in several regions, including Brazil [24, 25], Thailand, and Vietnam [26-28]. During the 2009 influenza H1N1 pandemic, additional countries, including Nicaragua [2], Puerto Rico [1] and India [29] reported cases of co-infection with DENV, resulting in severe disease [2]. Yet, whether and how co-infection with influenza and DENV affects pathogenesis remains unclear.

Based on these clinical observations, we established a mouse model to study how co-infection with influenza and DENV affects immune responses and pathogenesis. We used a 2009 pandemic influenza A virus H1N1 clinical isolate from Nicaragua (hereafter "H1N1") without adaptation to mice and the DENV2 strain D220 (hereafter "DENV"). D220 was derived via passaging between mosquito cells and immunodeficient mice, resulting in defined mutations and a potentially lethal vascular leak syndrome in mice that resembles key features of severe dengue in humans [30, 31]. We establish here that co-infection of influenza H1N1 followed two days later by DENV augments pathogenesis and induces lethal disease at otherwise sublethal

virus doses and define a mechanism that explains the increased severity via altered host responses.

Results

Co-infection with influenza H1N1 and DENV causes lethal disease.

We established a mouse model to determine whether co-infection with H1N1 and DENV affects immune responses and pathogenesis. WT mice were susceptible to infection with the Nicaraguan pandemic H1N1 clinical isolate without prior adaptation, as determined in dose-response experiments (Supporting information Fig. 1). Inoculating WT mice with 15,000 egg infectious dose-50 (EID_{50}) of H1N1 per gram of body weight for females caused 5-10% weight loss and sublethal disease (Supporting information Fig. 1). Previous studies showed that DENV proteins block IFN signaling in humans but not in mice [32, 33], and thus WT mice do not support DENV replication [34]. We demonstrate here that also in the context of a sublethal H1N1 infection, WT mice did not show additional weight loss or morbidity when infected intravenously with a high dose of 10^7 plaque forming units (PFU) DENV, 2 days prior or 2 days after infection with a sublethal dose of H1N1 (Supporting information Fig. 1).

Given that WT mice are resistant to DENV infection, we used *Ifnar*$^{-/-}$ mice that are susceptible to DENV infection and, after inoculation of a high DENV dose of 10^6-10^7 PFU or during antibody-enhanced infection, develop key features of severe human dengue disease, such as systemic vascular leak [30, 31, 35]. After intravenous infection with a lower dose of $3x10^5$ PFU of DENV alone, *Ifnar*$^{-/-}$ mice lost ~10% weight (Fig. 1A), displayed only mild signs of morbidity (Supporting information Fig. 1), and developed sublethal disease (Fig. 1B). For influenza virus, *Ifnar*$^{-/-}$ mice were as susceptible to infection with H1N1 alone as WT mice, showing similar weight loss (Figs. 1A and Supporting information Fig. 1) and sublethal disease. In contrast, co-infection of *Ifnar*$^{-/-}$ mice with H1N1 followed 2 days later by DENV significantly increased morbidity (Supporting information Fig. 1) and caused severe weight loss (Fig. 1A) and 90% lethality on day 5 (Fig. 1B). Autopsies revealed fluid accumulation in stomach and intestine that is indicative of systemic plasma leak [30, 35]. Sequential infection with DENV followed two days later by H1N1 caused only moderate weight loss and 44% lethality. Due to the more severe disease outcome, we focused on co-infecting *Ifnar*$^{-/-}$ mice with H1N1 followed by DENV, which we refer to hereafter as "co-infection" or "H1N1–DENV".

Co-infection with H1N1 increases DENV titers.

To examine the cause of exacerbated pathogenesis, we measured genomic viral RNA titers via qRT-PCR. *Ifnar*$^{-/-}$ mice displayed similar H1N1 titers in the lungs during co-infection or following infection with H1N1 alone, 4 days after inoculation with H1N1 and 2 days after inoculation with DENV (Fig. 2A). In contrast, co-infection significantly increased DENV titers in

the lung (3.1-fold), liver (4.2-fold), and spleen (10.5-fold) (Fig. 2B). Small intestine or serum did not contain detectable H1N1 but contained DENV at levels that were similar during co-infection or infection with DENV alone (Supporting information Fig. 2). Co-infection thus led to a significant increase in DENV titers in lung, liver, and spleen that likely contributed to the exacerbated disease phenotype and death that occurred one day after virus titers were analyzed. In addition, the lung was the only tissue in which both viruses were present (Fig. 2).

Co-infection with H1N1 and DENV induces severe pneumonia.

To determine whether the presence of both viruses caused increased pathology, we examined lungs via histology and immunohistochemistry. During co-infection or infection with H1N1 alone, lungs of *Ifnar*$^{-/-}$ mice displayed necrosis within the airway epithelium, as identified via H&E stains (Fig. 3A). In contrast, only lungs of co-infected mice developed severe pneumonia, characterized by marked necrosis of alveoli (Fig. 3A). Histology further revealed that co-infected lungs contained more neutrophils and less cells with a monocyte/macrophage phenotype compared to lungs that were infected with DENV alone (Fig. 3A). Livers of co-infected mice contained mildly increased numbers of neutrophils in the sinusoids with occasional single cell hepatocellular necrosis that was not observed in the mice infected with H1N1 or DENV alone (Supporting information Fig. 3). Lesions in the liver of co-infected mice were not pronounced enough to be the cause of lethal disease. Spleens of co-infected mice and mice infected with DENV alone showed hyperplastic germinal centers, which are indicative of B cell proliferation (Supporting information Fig. 3). The splenic red pulp in co-infected mice and mice infected with DENV alone contained increased numbers of neutrophils and monocytes / macrophages (Supporting information Fig. 3). Co-infected lungs displayed positive staining for H1N1 antigen in epithelial cells of the airways (Fig. 3B). The areas of severe necrosis of alveoli were, however, negative for H1N1 antigen (Fig. 3B). Overall, livers and spleens of co-infected mice only showed mild lesions, making severe pneumonia a second hallmark of co-infection, in addition to increased DENV titers, and a likely cause of weight loss and mortality.

Lungs of co-infected mice express partial or intermediate responses as compared to single infection.

The severe pneumonia and presence of both viruses in co-infected lungs led us to hypothesize that altered immune responses may contribute to lung pathology. We compared host mRNA responses in the lungs of single or co-infected *Ifnar*$^{-/-}$ mice via nCounter analysis (nanoString). Hybridization with gene-specific oligonucleotide probes (conjugated to 6-color bar codes) detected 179 selected genes that represent various inflammatory pathways. Two sets of genes were expressed significantly differently in co-infected compared to singly-infected lungs (Fig. 4A). We identified 18 genes with differential expression between co-infection and infection with H1N1 alone (Fig. 4B) and 25 genes with differential expression between co-infection and infection with DENV alone (Fig. 4C) that were changed more than 2-fold compared to PBS controls. Even though the expression of these genes was significantly different from single infection with one virus, they were expressed at intermediate levels or similarly to infection

with the other virus. Only three genes (*Il6ra*, *Bcl6*, *Csf2*) were differentially expressed during co-infection compared to infection with H1N1 alone and infection with DENV alone (Fig. 4D), but expression of these genes changed less than 2-fold. Conversely, a separate set of 54 genes changed significantly during infection with H1N1 and/or DENV compared to PBS controls but were not expressed significantly differently during co-infection and infection with either virus alone; thus, these genes were part of a common response to infection. All analyzed genes that are not reported in Fig. 4 are listed in Supporting information Table 1. Together, these results indicate that gene expression in the lungs of co-infected mice resembles partial or intermediate responses to infection with either H1N1 or DENV alone. Because infection with either virus alone (at the doses selected) caused relatively mild, sublethal disease, we presume that these responses are beneficial. Surprisingly, co-infection did not lead to a more pronounced expression of genes that were already expressed during single infection and that could have caused mortality during co-infection. In contrast, a "tug of war" between the immune responses to infection with H1N1 or DENV resulted in only partial or intermediate responses that were not sufficient to fight co-infection with both viruses and may instead have caused severe immunopathology.

The combined partial responses to co-infection generated a unique pattern of mRNA expression, which was further revealed via unbiased clustering (Figs. 4E, S4). The Pearson correlation was used as a distance metric and Wards minimum distance as the linkage method. All but two lung samples clustered according to their schedule of inoculation (Figs. 4E, S4), confirming that inoculation with DENV alone, H1N1 alone, H1N1–DENV, or PBS induced unique host RNA responses that resulted in unbiased clustering. We annotated most differentially expressed genes into families according to function. Genes that were differentially expressed between co-infection and H1N1 infection but were shared between co-infection and DENV infection (Fig. 4B) are involved in innate viral recognition, DC activation, or stress responses (Fig. 4F). Two different sets of genes involved in cytokine signaling were expressed either during infection with DENV alone and co-infection or during infection with H1N1 alone and co-infection (Fig. 4F). Genes that were differentially expressed between co-infection and DENV infection but were shared between co-infection and H1N1 infection (Fig. 4C) form part of the complement system or are chemokines that regulate the recruitment of inflammatory cells (Fig. 4F). In particular, chemokines that serve to recruit monocytes via CCR2 (*Ccl2,7,8*), neutrophils via CXCR2 (*Cxcl1,3,5*), or NK and effector T cells via CXCR3 (*Cxcl10*) were differentially regulated. Differences in cytokine responses, complement activation, or cell recruitment may thus have caused the severe pathology that we observed during co-infection.

Co-infected lungs are deficient in monocyte recruitment.

Due to the differential regulation of several chemokines in the lungs of co-infected mice, we performed flow cytometric analysis of inflammatory cell recruitment, 4 days after H1N1 and/or 2 days after DENV infection. Ly6C^{high} monocytes are commonly recruited from the blood to inflamed tissues, where they produce cytokines and phagocytize pathogens as well as damaged cells [36]. Of all cell types and tissues analyzed, significantly less recruitment of Ly6C^{high}

monocytes to the lung was the only detectable difference during co-infection versus infection with DENV alone (Fig. 5A, B). These results are in line with our histological analyses described above (Fig. 3). The decreased number of monocytes in the lung was not due to increased apoptosis, as measured via Zombie Aqua staining. Monocytes were also recruited to the spleen and liver, but no significant differences existed between co-infection and infection with DENV alone (Figs. 5B, S5). The bone marrow contained comparable numbers of monocytes in all conditions, including steady state, indicating that the reservoir of monocytes was not depleted during infection (Figs. 5B, S5). Little or no monocyte recruitment occurred to any tissue examined 4 days after infection with H1N1 alone (Fig. 5B, S5). In addition, significant numbers of $Ly6G^+$ neutrophils were recruited to the lung, spleen and liver during co-infection or infection with DENV alone, but no significant differences existed between these conditions (Figs. 5A, C, S5). The bone marrow was significantly depleted of neutrophils during co-infection and infection with DENV alone (Figs. 5C, S5). In addition, $CD4^+$ or $CD8^+$ T cells decreased during co-infection and infection with DENV alone, and no recruitment of NK cells to the lung was observed (Supporting information Fig. 5). Overall, co-infected mice developed severe pathogenesis and failed to recruit monocytes to lungs.

Monocytes play a beneficial role in the host response to co-infection.

Based on the lack of monocyte recruitment to the lungs of co-infected mice, which developed severe pathogenesis, we hypothesized that monocytes play a beneficial role in the response to co-infection. Adoptive transfer of WT monocytes into *Ifnar*$^{-/-}$ recipients significantly delayed death and increased survival of co-infected mice (Fig. 6A). In contrast, monocyte depletion accelerated pathogenesis, and co-infected mice that were treated with anti-CCR2 antibody succumbed to infection faster than isotype-control treated mice (Fig. 6B). For neutrophils, an equivalent adoptive transfer and depletion strategy using anti-Ly6G antibody did not affect the survival of co-infected mice (Supporting information Fig. 6). Monocytes thus play a beneficial role in the systemic host response during co-infection with H1N1 and DENV, and the lack of monocyte recruitment to the co-infected lung likely contributed to exacerbating pathogenesis.

Discussion

Using a new mouse model, we establish here that co-infection with pandemic influenza H1N1 followed two days later by DENV exacerbated pathogenesis and induced lethal disease in *Ifnar*$^{-/-}$ mice. In addition to increasing systemic DENV titers, co-infection induced severe pneumonia, impaired host mRNA responses in the lung, and blocked the recruitment of monocytes.

Our finding that co-infection augmented disease severity in mice extends the clinical reports that initiated our study. Simultaneous circulation or co-infection with seasonal influenza A virus and DENV1-4 were reported in India [37], Puerto Rico [38], and Thailand [39]. In addition, several reports confirmed cases of co-infection with 2009 pandemic H1N1 and DENV-

1 or DENV-3, in some instances leading to severe disease [1, 2, 4]. Here we establish a causal relationship between co-infection and increased disease severity, as H1N1–DENV co-infected mice succumbed to infection at otherwise sublethal virus doses. Consequently, co-infection is a risk factor for severe disease in tropical regions, such as Brazil [24, 25], Thailand, and Vietnam [26-28], where influenza and dengue viruses regularly co-circulate.

Co-infection increased DENV titers in the spleen, liver, and lung, suggesting that host responses were not able to control systemic DENV titers. The accumulation of fluid in the stomach and intestine that co-infected mice developed were similar to the systemic vascular leak syndrome that we commonly observe in our mouse model after lethal infection with higher DENV doses or during antibody-enhanced infection with a low viral dose [30, 31, 35]. Systemically increased DENV titers have thus likely contributed to exacerbate pathogenesis during co-infection.

Our data are in line with reports showing that H1N1 and DENV can both infect the lung. We confirm that influenza A virus targets epithelial cells of the respiratory tract [7] and confirm the presence of DENV in the serum, spleen, liver, intestine, and lung. Previous studies have identified monocytes, macrophages, and DCs as main targets of DENV replication in these tissues [12, 13]. We establish here that the lung of co-infected mice was the only tissue that contained, both, H1N1 and DENV.

Influenza as well as dengue patients can experience lung pathology. Vascular leak in dengue shock cases can lead to pleural effusion in the lungs [14]. Intravenous administration of fluids is an effective therapy to compensate for plasma leak; however, excessive or too rapid intravenous fluids can also lead to pleural effusion [14, 40]. Other lung abnormalities are less common in dengue [41] and mostly occur with co-morbidities [14, 42]. Most severe cases of pneumonia resulting from influenza A infection are due to opportunistic bacterial infections that usually occur after influenza A virus is cleared but still has immunomodulatory effects [23]. We determined here that *Ifnar*$^{-/-}$ mice developed severe pneumonia with necrosis of alveoli only during co-infection. These findings have implications for diagnostic or therapeutic approaches. Patients who present with severe respiratory symptoms should be tested for influenza and DENV in regions where both viruses co-circulate. The hypothesized interaction between H1N1 and DENV infections has already triggered adaptation of treatment protocols. The Ministry of Health guidelines in Nicaragua during the 2009 H1N1 pandemic called for early but moderate fluid therapy that may have prevented more severe disease during the H1N1 pandemic, which overlapped with the dengue epidemic that year [2, 3]. Vaccination may be another option to lower the risk of severe co-infection.

As we did not observe T-cell recruitment to the lung and mice succumbed to co-infection by 5 days after infection, more immediate immune responses may have contributed to exacerbate pathogenesis. Monocytes can play beneficial or detrimental roles during viral infections. Early after DENV transmission, monocytes are recruited to the dermis and serve as targets for DENV replication [10]. Further, DENV-infected monocytes were found in the blood of

acute dengue patients [43]. While these studies suggest a detrimental role for DENV-infected monocytes in dengue pathogenesis, non-infected monocyte-derived DCs pulsed with DENV envelope protein stimulated DENV-specific memory T cell responses [44], and $CD14^+$ $CD16^+$ monocytes promoted DENV-specific B-cell responses [45]. During infection with influenza A virus, CCR2-deficient mice lacked monocyte recruitment to the lung and developed less immunopathology and mortality than WT mice [46]. In contrast, CCL2/7-mediated recruitment of monocyte-derived DCs to the influenza-infected lung supported virus-specific $CD8^+$ T cells and virus clearance [47]. Thus, while excessive monocyte recruitment causes immunopathology, moderate monocyte responses are necessary to defend against influenza virus [36]. In our study, ligands for CCR2 (*Ccl2, -7*, *-8*) were upregulated during co-infection and H1N1 infection, but only infection with DENV alone led to significant recruitment of monocytes. Lack of monocyte recruitment to the lung was the only significant difference in the cellular immune response between infection with DENV alone and co-infection, of which only the latter caused severe pneumonia. Because systemic depletion of monocytes accelerated pathogenesis and adoptive transfer rescued some mice from lethal disease, we conclude that monocytes play a beneficial role in the systemic response to co-infection.

A limited number of studies have addressed the role of neutrophils in dengue pathogenesis, showing recruitment of neutrophils to the DENV-infected dermis [10] or degranulation of neutrophils in dengue patients [48]. We observed neutrophil recruitment to the lung and increased expression of *Il8rb* (*Cxcr2*), the main receptor regulating neutrophil migration, during co-infection or infection with DENV alone. The cognate ligands (*Cxcl1*, *-3*, *-5*) were upregulated during co-infection or infection with H1N1 alone. The relatively mild infection with H1N1 alone likely explains why no increase in monocytes or neutrophils was detectable in the lung 4 days post-inoculation. Moderate recruitment of neutrophils to the lung was beneficial for influenza-specific $CD8^+$ T cell responses [49], but excessive recruitment of neutrophils resulted in pathogenesis [50]. Histology revealed more neutrophils in co-infected lungs compared to infection with DENV alone, while flow cytometry did not detect significant differences. Modulating neutrophil numbers via adoptive transfer of neutrophils or depletion did not affect disease outcome during co-infection. Thus, whether neutrophils contributed to augment lung pathology remains to be determined.

Additional pathways likely contributed to lung pathology. On the one hand, co-infection induced a partial gene expression profile that was similar to infection with DENV alone, increasing innate viral recognition (*Tlr6*, *Myd88*), decreasing DC activation (*CD40lg*, *Csf2*, *Ccr7*), and increasing cellular stress responses (*Maff*, *Itgb2*, *Hspb1*). On the other hand, co-infection induced a gene expression profile that was partially similar to infection with H1N1 alone, increasing cytokine responses (*Il6*, *Tnf*, *Il1rn*) that take part in DENV pathogenesis [15] and upregulating components of the complement system (*C1qa/b, C3ar1, C8b, Cfb*). Complement can neutralize DENV infection [51], contribute to dengue pathogenesis [52] or augment H1N1 pathogenesis via immune complexes [53]. We expected that co-infection would exacerbate the expression of inflammatory genes that would then cause mortality, as likely occurs after

inoculation with a lethal dose of one virus. Surprisingly, none of the examined genes was expressed significantly more pronounced compared to single infection even though co-infection significantly increased DENV titers. This gene expression profile suggests a "tug of war" between otherwise beneficial host responses against H1N1 or DENV infection. These partial responses fail to control DENV titers, instead causing immunopathology, tissue damage, and lethal disease.

Apart from worldwide reports of clinical co-infections [1, 2, 29], more distantly timed infections may affect pathogenesis. In Nicaragua, the 2009 H1N1 pandemic overlapped with the annual DENV epidemic [3]. Multivariate analysis adjusted for age, sex, and dengue immune status showed that cases in 2009/10 had a 2.6-fold higher risk of developing dengue with compensated shock than cases in the seasons 2005-09 or 2010/11, even though DENV3 was the dominant serotype from 2008-11 and the virus sequence did not change [3]. More individuals who carried H1N1-specific antibodies and thus had been infected with the pandemic strain since its recent introduction into Nicaragua presented with shock than individuals without prior exposure [3]. Longer-term effects of a H1N1 infection on innate or adaptive immune responses may thus help explain the large and atypical dengue epidemic that Nicaragua experienced in 2009/2010.

IFN signaling may further modulate the susceptibility to secondary virus infections. DENV NS2B3 and NS5 proteins [32, 54] and influenza virus NS1 [55] are strong suppressors of the IFN response in infected human cells. In contrast, DENV proteins are not able to suppress IFN signaling in mice [32], making WT mice resistant to DENV infection [10, 34]. Our finding that WT and *Ifnar*$^{-/-}$ mice were similarly susceptible to H1N1 infection may be strain-specific, as we used a Nicaraguan pandemic H1N1 isolate whereas prior studies have reported an increased susceptibility of *Ifnar*$^{-/-}$ mice to infection with influenza virus A/PR/8/34 or A/FM/1/47 (both H1N1) [56] but not to infection with strain X31 (H3N2) [57]. Our data that WT mice were resistant to DENV infection also after infection with H1N1 indicates that H1N1-mediated suppression of IFN signaling was not sufficient to allow for DENV replication, likely because both viruses mostly infect different cell types. *Ifnar*$^{-/-}$ mice mimic key features of human dengue disease [30, 31, 35] and currently are the best available model to study infection with H1N1 and DENV. Co-infection of *Ifnar*$^{-/-}$ mice led to strong upregulation of *Ifnb1* and *Stat1*, although the mice are deficient in IFNAR signaling. Our data thus show that co-infection of H1N1 and DENV can exacerbate pathogenesis independently of IFN signaling. Nevertheless, IFN-α/β-mediated signals may well play an additional role in co- or sequential infections with H1N1 and DENV in humans. Future studies in patients or refined animal models need to assess the role of IFNAR signaling in exacerbated disease severity during co-infection or after sequential H1N1–DENV infection [3].

In summary, we established that co-infection of pandemic H1N1 followed two days later by DENV caused lethal disease in *Ifnar*$^{-/-}$ mice. Immune responses during co-infection failed to control the pathogen burden, leading to the increased DENV titers that likely contributed to augment systemic pathogenesis. In addition, lungs generated only partial host-RNA responses

against infection with either virus that were not sufficient to fight co-infection and instead caused severe tissue damage. Co-infected lungs lacked the recruitment of monocytes that was part of a beneficial response and was characteristic of infection with DENV alone. Our findings provide novel insight into disease mechanism of co-infection and encourage prompt diagnostics, therapeutic intervention, and vaccination to prevent severe disease in regions where dengue and influenza viruses regularly co-circulate. Providing data on the largely understudied field of co-infections with acute viruses, our study should encourage further research on co-infections.

Materials and methods

Ethics statement

Mice were bred in the animal facility, and fertilized chicken eggs were incubated in the laboratories at the University of California, Berkeley. Experiments were performed strictly following guidelines of the American Veterinary Medical Association and the Guide for the Care and Use of Laboratory Animals of the National Institutes of Health. The University of California Berkeley's Animal Care and Use Committee pre-approved all experiments (protocol AUP-2014-08-6638).

Influenza virus

A clinical isolate of Influenza A virus A/NI/5227/2009 of the H1N1 subtype from the 2009 pandemic in Nicaragua (here termed H1N1) was expanded in embryonated chicken eggs, as previously described [58]. In brief, fertilized research grade eggs (Charles River) were incubated at 37.7°C at 63% relative humidity in a circulated-air incubator (2365 Hova-Bator, GQF), automatically turning the eggs every 12 h. On day 10, eggs with viable embryos (as tested via a light bulb candle) were used for infection. A hole was drilled above the air sac line and 100 µl of H1N1 in 10-fold serial dilutions in PBS with 2,000 units/ml Penicillin G, 200 units/ml Polymyxin B, and 0.4 mg/ml Streptomycin (Sigma) was injected into the allantoic fluid. After sealing the hole with paraffin wax and incubating for three more days, the unhatched chicken embryos were euthanized via cooling overnight at 4°C and puncturing the egg membranes. The allantoic fluid was harvested and tested for the presence of H1N1 via hemagglutination assay using 0.25% turkey red blood cells (Colorado Serum Co). Titers of H1N1 stocks were determined in embryonated chicken eggs and calculated as egg infectious dose-50 (EID_{50})/ml following the Reed-Muench method.

Dengue virus

The DENV2 stain D220 (here termed DENV) was previously derived from the Taiwanese clinical isolate PL046 via 20 passages between C6/36 *Ae. albopictus* cells and serum of 129/Sv mice deficient in IFN-α/β and -γ receptors, acquiring defined mutations that increase its virulence in

mice [30, 31]. DENV stocks were grown in C6/36 cells that were cultured at 28°C in M199 medium supplemented with 10% fetal bovine serum (FBS), 100 U/ml penicillin/streptomycin, and GlutaMax (LifeTechnologies) and infected with DENV for 2 h in serum-free RPMI 1640 medium and then adjusted to 2% FBS. Supernatants containing DENV were harvested on days 5 to 8, concentrated via Amicon Ultra-15 Centrifugal Filter Units (Millipore) with a 100 kDa molecular weight cut-off, and pooled at the last day of harvest [10]. Virus titers were determined via plaque assay using BHK-21 clone 15 cells cultured at 37°C and 5% CO_2 in α-MEM medium with 5% FBS, 100 U/ml penicillin/streptomycin, and GlutaMax (LifeTechnologies). Ten-fold serial dilutions of DENV stocks were used to inoculate BHK-21 cells in 12-well plates (Becton Dickinson) for 2 h before overlaying with 10% low-melting Agarose (Cambrex). After 7 days, the cells were fixed with 10% buffered formalin phosphate (Fisher Scientific) and stained with 2.5% crystal violet in 30% ethanol. DENV titers were calculated as plaque forming units (PFU)/ml.

Mice

Wild-type (WT) C57BL/6 mice were purchased from the Jackson Laboratory. C57BL/6 mice deficient in the IFN-α/β receptor-1 (*Ifnar*^{1tm1Agt}, here termed *Ifnar*$^{-/-}$) were obtained from Dr. Daniel Portnoy (University of California, Berkeley). Mice were infected with one virus or co-infected with H1N1 and DENV within two days of each other. Isoflurane-anesthetized female WT or *Ifnar*$^{-/-}$ mice received 15,000 EID_{50} H1N1 intranasally per gram body weight and males received 75,000 EID_{50}/g, each leading to a weight loss of 5-10%. *Ifnar*$^{-/-}$ mice received 3 x10^5 PFU DENV intravenously and WT mice 10^7 PFU DENV. Control mice received equivalent inoculations of PBS. Infected mice were weighed and monitored for morbidity using the standardized 5-point scale [10, 31]: 1, healthy; 2, mild signs of lethargy; 3, fur ruffling, hunched posture; 4, increased lethargy, limited mobility, ruffled fur, hunched posture; 5, moribund with minimal mobility and inability to reach food or water. Mice that lost >20% weight or became moribund were euthanized immediately for ethical reasons. Before collecting tissues for analysis, euthanized mice were perfused with PBS.

Quantification of virus genomes

Tissue samples were stored at -80°C in RNAlater (Ambion). A piece of <20 mg tissue was homogenized for 1 min with 1-mm zirconia-silica beads using a Mini-Beadbeater-8 (BiospecProducts). RNA was extracted from tissues using the RNeasy Mini Kit or from 20 µl serum using the QIAamp Viral RNA Mini Kit (Qiagen). For quantification of virus genomes via qRT-PCR, we used the pandemic influenza A H1N1-specific standard kit (Genesig) or DENV2 NS5 primers and probes (synthesized by Eurofins Operon), the Verso one-step qRT-PCR Kit (Thermo Scientific), and a 7300 Real-Time PCR System (Applied Biosystems). DENV2 NS5 primer and probe sequences were as follows: forward primer 5'ACA AGT CGA ACA ACC TGG TCC AT; reverse primer 5'GCC GCA CCA TTG GTC TTC TC; probe 5'-Fam TGG GAT TTC CTC CCA TGA TTC CAC TGG Tamra-Q. The Thermal Cycler was set to the following profile: reverse transcription at 50°C for 30 min, hot start at 95°C for 12.5 min, and 40-50 PCR cycles consisting

of denaturation at 95°C for 15 sec and annealing/extension at 60°C for 1 min. During quantification of virus titers, one out of *n*=11 co-infected mice had no detectable levels of H1N1 in the lungs and was omitted from the analysis due to unsuccessfully infection. The TaqMan Rodent *Gapdh* Control Reagent (Applied Biosystems) served to normalize virus genome equivalents to tissue *Gapdh* mRNA as a relative approximation for total cellular RNA. The *Gapdh* gene was stably expressed between all experimental groups, as determined via nCounter analysis (nanoString) described below.

nCounter gene mRNA expression

The nCounter GX Mouse Inflammation Kit was used to perform mRNA expression analysis in lung tissue of 179 genes that represent inflammatory pathways (nanoString). One hundred ng of RNA were hybridized overnight with gene-specific capture and detection probes that bind mRNA at exon-exon borders and carry 6-color barcodes for detection. Probe-mRNA complexes were then immobilized onto solid-support cartridges via the capture probes, and non-specific RNA was washed away. Without any amplification, mRNA copies were counted using the digital analyzer, and data were analyzed using the nSolver 2.0 software (nanoString). For normalization of RNA content between samples, six genes (*Cltc*, *Gapdh*, *Map2k1*, *Shc1*, *Ly96*, *Traf2*) with low variation overall and between experimental groups were selected based on the NormFinder algorithm V20. Genes with an average count <25 were excluded from further analysis (see Supporting information Table 1).

Histology & immunohistochemistry

Formalin-fixed tissues were embedded in paraffin, cut into 5-µm sections, and stained with Hematoxylin and Eosin (H&E). For staining H1N1 antigen, paraffin wax was removed using Bond Dewax solution (Leica), and antigen was retrieved via incubation for 5 min with Proteinase K (Dako). Then, primary influenza-A USSR H1N1-specific antibody (USBiological) was applied for 60 min, followed by rabbit anti-goat secondary antibody (Vector Labs) for 15 minutes and anti-rabbit horseradish peroxydase polymer (Leica) for 15 min at room temperature. Stained slides were visualized using the Bond Polymer Refine detection system with 3,3´-diaminobenzidine chromogen and hematoxylin counterstain (Leica). Histological sections were stained using the Bond-Max immunohistochemistry system (Leica) and imaged using the Eclipse 50i microscope (Nikon).

Flow cytometry

Lungs were washed in PBS, cut into small pieces using scissors in RPMI 1640 medium containing 10% FBS, and digested for 45 min in 1.6 mg/ml collagenase type-1 (LifeTechnologies) and 10 U/ml DNase-1 (Roche) at 37°C while shaking at 220 rotations per minute. Spleens and livers were squashed and digested in 1 mg/ml collagenase type-1 and 10 U/ml DNase-1 for 30 min at 37°C and 5% CO_2. Homogeneous cell suspensions were generated via pipetting and filtration through 100-µm nylon meshes (ELKO). Red blood cells of bone

marrow and spleen samples were lysed using Red Blood Cell Lysis Buffer (eBioscience). Staining samples with Zombie Aqua (BioLegend) excluded dead cells. Cell surface markers were stained using the following monoclonal antibodies (BioLegend or BD): B220 (RA3-6B2), CD11c (N418), CD11b (M1/70), CD45 (30-F11), Ly6C (AL21), Ly6G (1A8), MHC II (I-A/I-E, M5/114.15.2), which were conjugated to PacificBlue, Brilliant Violet 605, Alexa Fluor 488, PE, PE-CF594, Alexa Fluor 647, Alexa Fluor 700, APC-Cy7, or biotin. Cells stained with biotinylated antibodies were visualized using Brilliant Violet 605- or PE-Cy7-conjugated streptavidin (BioLegend). Data were recorded with an LSR Fortessa (BD) and analyzed using FlowJo 8.8.7 software (TreeStar).

Cell depletions

Co-infected (H1N1–DENV) *Ifnar*$^{-/-}$ mice were depleted of monocytes via inoculation of 20 μg anti-CCR2 (MC-21) antibody intraperitoneal on days 1, 2, 3, and 4 after H1N1 infection [59]. To deplete neutrophils, 500 μg of anti-Ly6G (1A8) antibody (BioXCell) was inoculated intraperitoneal on days 1 and 3. Control animals were injected with equivalent amounts of rat IgG2b isotype-matched control antibody (BioXCell or UCSF).

Adoptive transfers

Bone marrow cells were obtained by crushing femurs, tibias and vertebral columns of WT mice with mortar and pestle in PBS without Ca^{2+}/Mg^{2+} containing 2% FBS and 2 mM EDTA. After centrifugation on Ficoll-Paque (GE Healthcare), cells from the interphase were used for monocyte isolation, and cells from the pellet for neutrophil isolation. For neutrophils, red blood cells were lysed using Red Blood Cell Lysis Buffer (eBioscience) in the presence of 20 U/ml DNase-1 (Roche) to prevent clumping. Monocytes or neutrophils were each isolated using MACS Kits (Miltenyi) via depletion of other cell types, and adding 5% normal rat serum served to block nonspecific binding. MHCII$^-$ CD11b$^+$ Ly6G$^-$ Ly6C$^+$ monocytes were enriched from an average of 12% in the bone marrow to 82% and 88% in two experiments; and MHCII$^-$ CD11b$^+$ Ly6G$^+$ neutrophils were enriched from an average of 54% in the bone marrow to 92% and 98%, respectively. A total of 9-10 x10^6 monocytes or 12-14 x10^6 neutrophils were transferred intravenously into co-infected *Ifnar*$^{-/-}$ mice on day 2 after H1N1 infection.

Statistical analysis

Statistical significances for survival data were determined using the Log-rank (Mantel-Cox) test. Unpaired t-tests were used to determine significant differences for weight loss, gene mRNA expression, or flow cytometry. Analyses that included more than two experimental groups were performed using one-way ANOVA. Unpaired Mann-Whitney tests were used to determine significant differences for non-parametric data, such as morbidity or viral load. The Holm-Sidak method was used to correct for multiple comparisons when comparing mRNA expression of infected samples to PBS controls. P-values were considered significant at values <0.05. Data were plotted and analyzed using Prism 6.0 (GraphPad) software.

Acknowledgements

We would like to thank Andrew Frando for help in establishing the mouse model and Kalani Ratnasiri and Angelo Torres for maintaining the mouse colony. We thank Andrea Lawrence for histological analyses and Kelli Boyd for serving as pathologist. We thank Josefina Coloma for helpful scientific discussion and grants management and Stephen Popper for advice on gene expression data. This work was supported by an Innovation Grant (#3274) from the UBS Optimus Foundation awarded to the Sustainable Sciences Institute and the University of California, Berkeley (EH). MAS and EH designed the experiments; MAS, KNG, SS, JP, and LBT performed the experiments, analyzed and interpreted data; JP, MM, FPP, and EH provided material; MAS and EH wrote the manuscript.

Conflict of interest

The authors declare no commercial or financial conflict of interest.

References

1 **Lopez Rodriguez, E., Tomashek, K. M., Gregory, C. J., Munoz, J., Hunsperger, E., Lorenzi, O. D., Irizarry, J. G. and Garcia-Gubern, C.,** Co-infection with dengue virus and pandemic (H1N1) 2009 virus. *Emerg Infect Dis* 2010. **16**: 882-884.

2 **Perez, M. A., Gordon, A., Sanchez, F., Narvaez, F., Gutierrez, G., Ortega, O., Nunez, A., Harris, E. and Balmaseda, A.,** Severe coinfections of dengue and pandemic influenza A H1N1 viruses. *Pediatr Infect Dis J* 2010. **29**: 1052-1055.

3 **Gutierrez, G., Standish, K., Narvaez, F., Perez, M. A., Saborio, S., Elizondo, D., Ortega, O., Nunez, A., Kuan, G., Balmaseda, A. and Harris, E.,** Unusual dengue virus 3 epidemic in Nicaragua, 2009. *PLoS Negl Trop Dis* 2011. **5**: e1394.

4 **Behera, V., Naithani, N., Nizami, A. and Ranjan, R.,** A rare case of dengue and H1N1 co-infection: A deadly duo. *Lung India* 2015. **32**: 299-300.

5 **WHO,** Influenza (Seasonal). Fact sheet No 211. 2014.

6 **Webster, R. G., Bean, W. J., Gorman, O. T., Chambers, T. M. and Kawaoka, Y.,** Evolution and ecology of influenza A viruses. *Microbiol Rev* 1992. **56**: 152-179.

7 **Weinheimer, V. K., Becher, A., Tonnies, M., Holland, G., Knepper, J., Bauer, T. T., Schneider, P., Neudecker, J., Ruckert, J. C., Szymanski, K., Temmesfeld-Wollbrueck, B., Gruber, A. D., Bannert, N., Suttorp, N., Hippenstiel, S., Wolff, T. and Hocke, A. C.,**

Influenza A viruses target type II pneumocytes in the human lung. *J Infect Dis* 2012. **206**: 1685-1694.

8 **Dawood, F. S., Iuliano, A. D., Reed, C., Meltzer, M. I., Shay, D. K., Cheng, P. Y., Bandaranayake, D., Breiman, R. F., Brooks, W. A., Buchy, P., Feikin, D. R., Fowler, K. B., Gordon, A., Hien, N. T., Horby, P., Huang, Q. S., Katz, M. A., Krishnan, A., Lal, R., Montgomery, J. M., Molbak, K., Pebody, R., Presanis, A. M., Razuri, H., Steens, A., Tinoco, Y. O., Wallinga, J., Yu, H., Vong, S., Bresee, J. and Widdowson, M. A.,** Estimated global mortality associated with the first 12 months of 2009 pandemic influenza A H1N1 virus circulation: a modelling study. *Lancet Infect Dis* 2012. **12**: 687-695.

9 **Bhatt, S., Gething, P. W., Brady, O. J., Messina, J. P., Farlow, A. W., Moyes, C. L., Drake, J. M., Brownstein, J. S., Hoen, A. G., Sankoh, O., Myers, M. F., George, D. B., Jaenisch, T., Wint, G. R., Simmons, C. P., Scott, T. W., Farrar, J. J. and Hay, S. I.,** The global distribution and burden of dengue. *Nature* 2013. **496**: 504-507.

10 **Schmid, M. A. and Harris, E.,** Monocyte recruitment to the dermis and differentiation to dendritic cells increases the targets for dengue virus replication. *PLoS Pathog* 2014. **10**: e1004541.

11 **Cerny, D., Haniffa, M., Shin, A., Bigliardi, P., Tan, B. K., Lee, B., Poidinger, M., Tan, E. Y., Ginhoux, F. and Fink, K.,** Selective susceptibility of human skin antigen presenting cells to productive dengue virus infection. *PLoS Pathog* 2014. **10**: e1004548.

12 **Balsitis, S. J., Coloma, J., Castro, G., Alava, A., Flores, D., McKerrow, J. H., Beatty, P. R. and Harris, E.,** Tropism of dengue virus in mice and humans defined by viral nonstructural protein 3-specific immunostaining. *Am J Trop Med Hyg.* 2009. **80**: 416-424.

13 **Prestwood, T. R., May, M. M., Plummer, E. M., Morar, M. M., Yauch, L. E. and Shresta, S.,** Trafficking and replication patterns reveal splenic macrophages as major targets of dengue virus in mice. *J Virol* 2012. **86**: 12138-12147.

14 **WHO,** *Dengue guidelines for diagnosis, treatment, prevention and control. Third edition.* World Health Organization, Geneva: 2009.

15 **Guzman, M. G. and Harris, E.,** Dengue. *Lancet* 2015. **385**: 453-465.

16 **Halstead, S. B.,** Immune enhancement of viral infection. *Prog Allergy* 1982. **31**: 301-364.

17 **Blackley, S., Kou, Z., Chen, H., Quinn, M., Rose, R. C., Schlesinger, J. J., Coppage, M. and Jin, X.,** Primary human splenic macrophages, but not T or B cells, are the principal target cells for dengue virus infection in vitro. *J Virol* 2007. **81**: 13325-13334.

18 **Rothman, A. L.,** Immunity to dengue virus: a tale of original antigenic sin and tropical cytokine storms. *Nat Rev Immunol* 2011. **11**: 532-543.

19 **Magalhaes, B. M., Siqueira, A. M., Alexandre, M. A., Souza, M. S., Gimaque, J. B., Bastos, M. S., Figueiredo, R. M., Melo, G. C., Lacerda, M. V. and Mourao, M. P.,** P. vivax malaria and dengue fever co-infection: a cross-sectional study in the Brazilian Amazon. *PLoS Negl Trop Dis* 2014. **8**: e3239.

20 **Taraphdar, D., Sarkar, A., Mukhopadhyay, B. B. and Chatterjee, S.,** A comparative study of clinical features between monotypic and dual infection cases with Chikungunya virus and dengue virus in West Bengal, India. *Am J Trop Med Hyg.* 2012. **86**: 720-723.

21 **Dupont-Rouzeyrol, M., O'Connor, O., Calvez, E., Daures, M., John, M., Grangeon, J. P. and Gourinat, A. C.,** Co-infection with Zika and dengue viruses in 2 patients, New Caledonia, 2014. *Emerg Infect Dis* 2015. **21**: 381-382.

22 **See, K. C., Phua, J., Yip, H. S., Yeo, L. L. and Lim, T. K.,** Identification of concurrent bacterial infection in adult patients with dengue. *Am J Trop Med Hyg.* 2013. **89**: 804-810.

23 **Kash, J. C., Walters, K. A., Davis, A. S., Sandouk, A., Schwartzman, L. M., Jagger, B. W., Chertow, D. S., Li, Q., Kuestner, R. E., Ozinsky, A. and Taubenberger, J. K.,** Lethal synergism of 2009 pandemic H1N1 influenza virus and Streptococcus pneumoniae coinfection is associated with loss of murine lung repair responses. *MBio* 2011. **2**.

24 **Alonso, W. J., Viboud, C., Simonsen, L., Hirano, E. W., Daufenbach, L. Z. and Miller, M. A.,** Seasonality of influenza in Brazil: a traveling wave from the Amazon to the subtropics. *Am J Epidemiol* 2007. **165**: 1434-1442.

25 **Teixeira, M. G., Siqueira, J. B., Jr., Ferreira, G. L., Bricks, L. and Joint, G.,** Epidemiological trends of dengue disease in Brazil (2000-2010): a systematic literature search and analysis. *PLoS Negl Trop Dis* 2013. **7**: e2520.

26 **Chittaganpitch, M., Supawat, K., Olsen, S. J., Waicharoen, S., Patthamadilok, S., Yingyong, T., Brammer, L., Epperson, S. P., Akrasewi, P. and Sawanpanyalert, P.,** Influenza viruses in Thailand: 7 years of sentinel surveillance data, 2004-2010. *Influenza Other Respir Viruses* 2012. **6**: 276-283.

27 **Campbell, K. M., Lin, C. D., Iamsirithaworn, S. and Scott, T. W.,** The complex relationship between weather and dengue virus transmission in Thailand. *Am J Trop Med Hyg.* 2013. **89**: 1066-1080.

28 **Do, T. T., Martens, P., Luu, N. H., Wright, P. and Choisy, M.,** Climatic-driven seasonality of emerging dengue fever in Hanoi, Vietnam. *BMC Public Health* 2014. **14**: 1078.

29 **Borthakur, B., Panwar, D., Garg, R. and Pawar, M.,** Viral co-infection with dengue and H1N1 virus in a critical care setting. *J Anaesthesiol Clin Pharmacol* 2011. **27**: 236-238.

30 **Shresta, S., Sharar, K. L., Prigozhin, D. M., Beatty, P. R. and Harris, E.,** A murine model for dengue lethal disease with increased vascular permeability. *J Virol* 2006. **80**: 10208-10217.

31 **Orozco, S., Schmid, M. A., Parameswaran, P., Lachica, R., Henn, M. R., Beatty, R. and Harris, E.,** Characterization of a model of lethal dengue virus 2 infection in C57BL/6 mice deficient in the alpha/beta interferon receptor. *J Gen Virol* 2012. **93**: 2152-2157.

32 **Ashour, J., Morrison, J., Laurent-Rolle, M., Belicha-Villanueva, A., Plumlee, C. R., Bernal-Rubio, D., Williams, K. L., Harris, E., Fernandez-Sesma, A., Schindler, C. and Garcia-Sastre, A.,** Mouse STAT2 restricts early dengue virus replication. *Cell Host Microbe* 2010. **8**: 410-421.

33 **Aguirre, S., Maestre, A. M., Pagni, S., Patel, J. R., Savage, T., Gutman, D., Maringer, K., Bernal-Rubio, D., Shabman, R. S., Simon, V., Rodriguez-Madoz, J. R., Mulder, L. C., Barber, G. N. and Fernandez-Sesma, A.,** DENV inhibits type I IFN production in infected cells by cleaving human STING. *PLoS Pathog* 2012. **8**: e1002934.

34 **Shresta, S., Kyle, J. L., Snider, H. M., Basanavapatna, M., Beatty, R. and Harris, E.,** Interferon-dependent immunity is essential for resistance to primary dengue virus infection in mice, whereas T and B cell-dependent immunity is less critical. *J Virol* 2004. **78**: 2701-2710.

35 **Balsitis, S. J., Williams, K. L., Lachica, R., Flores, D., Kyle, J. L., Mehlhop, E., Johnson, S., Diamond, M. S., Beatty, P. R. and Harris, E.,** Lethal antibody enhancement of dengue disease in mice is prevented by Fc modification. *PLoS Pathog* 2010. **6**: e1000790.

36 **Shi, C. and Pamer, E. G.,** Monocyte recruitment during infection and inflammation. *Nat Rev Immunol* 2011. **11**: 762-774.

37 **Myers, R. M., Varkey, M. J., Reuben, R., Jesudass, E. S. and Benjamin, B.,** The 1968 outbreak of dengue in Vellore, Southern India. *Am J Public Health* 1971. **61**: 1379-1391.

38 **Morens, D. M., Rigau-Perez, J. G., Lopez-Correa, R. H., Moore, C. G., Ruiz-Tiben, E. E., Sather, G. E., Chiriboga, J., Eliason, D. A., Casta-Velez, A. and Woodall, J. P.,** Dengue in Puerto Rico, 1977: public health response to characterize and control an epidemic of multiple serotypes. *Am J Trop Med Hyg.* 1986. **35**: 197-211.

39 **Silarug, N., Foy, H. M., Kupradinon, S., Rojanasuphot, S., Nisalak, A. and Pongsuwant, Y.,** Epidemic of fever of unknown origin in rural Thailand, caused by influenza A (H1N1) and dengue fever. *Southeast Asian J Trop Med Public Health* 1990. **21**: 61-67.

40 **Vaughn, D. W., Green, S., Kalayanarooj, S., Innis, B. L., Nimmannitya, S., Suntayakorn, S., Endy, T., Raengsakulrach, B., Rothman, A. L., Ennis, F. A. and Nisalak, A.,** Dengue viremia titer, antibody response pattern, and virus serotype correlate with disease severity. *J Infect Dis* 2000. **181**: 2-9.

41 **Rodrigues, R. S., Brum, A. L., Paes, M. V., Povoa, T. F., Basilio-de-Oliveira, C. A., Marchiori, E., Borghi, D. P., Ramos, G. V. and Bozza, F. A.,** Lung in dengue: computed tomography findings. *PLoS ONE* 2014. **9**: e96313.

42 **Povoa, T. F., Alves, A. M., Oliveira, C. A., Nuovo, G. J., Chagas, V. L. and Paes, M. V.,** The pathology of severe dengue in multiple organs of human fatal cases: histopathology, ultrastructure and virus replication. *PLoS ONE* 2014. **9**: e83386.

43 **Durbin, A., Vargas, M. J., Thumar, B., Hammond, S. N., Gordon, G., Rocha, C., Balmaseda, A. and Harris, E.,** Phenotyping of peripheral blood mononuclear cells during acute dengue illness demonstrates infection and increased activation of monocytes in severe cases compared to classic dengue fever. *Virology* 2008. **376**: 429-435.

44 **Sun, P., Beckett, C., Danko, J., Burgess, T., Liang, Z., Kochel, T. and Porter, K.,** A dendritic cell-based assay for measuring memory T cells specific to dengue envelope proteins in human peripheral blood. *J Virol Methods* 2011. **173**: 175-181.

45 **Kwissa, M., Nakaya, H. I., Onlamoon, N., Wrammert, J., Villinger, F., Perng, G. C., Yoksan, S., Pattanapanyasat, K., Chokephaibulkit, K., Ahmed, R. and Pulendran, B.,** Dengue Virus Infection Induces Expansion of a CD14(+)CD16(+) Monocyte Population that Stimulates Plasmablast Differentiation. *Cell Host Microbe* 2014. **16**: 115-127.

46 **Lin, K. L., Suzuki, Y., Nakano, H., Ramsburg, E. and Gunn, M. D.,** CCR2+ monocyte-derived dendritic cells and exudate macrophages produce influenza-induced pulmonary immune pathology and mortality. *J Immunol* 2008. **180**: 2562-2572.

47 **Aldridge, J. R., Jr., Moseley, C. E., Boltz, D. A., Negovetich, N. J., Reynolds, C., Franks, J., Brown, S. A., Doherty, P. C., Webster, R. G. and Thomas, P. G.,** TNF/iNOS-producing dendritic cells are the necessary evil of lethal influenza virus infection. *Proc Natl Acad Sci U S A* 2009. **106**: 5306-5311.

48 **Juffrie, M., van Der Meer, G. M., Hack, C. E., Haasnoot, K., Sutaryo, Veerman, A. J. and Thijs, L. G.,** Inflammatory mediators in dengue virus infection in children: interleukin-8 and its relationship to neutrophil degranulation. *Infect Immun* 2000. **68**: 702-707.

49 **Lim, K., Hyun, Y. M., Lambert-Emo, K., Capece, T., Bae, S., Miller, R., Topham, D. J. and Kim, M.,** Neutrophil trails guide influenza-specific CD8(+) T cells in the airways. *Science* 2015. **349**: aaa4352.

50 **Narasaraju, T., Yang, E., Samy, R. P., Ng, H. H., Poh, W. P., Liew, A. A., Phoon, M. C., van Rooijen, N. and Chow, V. T.,** Excessive neutrophils and neutrophil extracellular traps contribute to acute lung injury of influenza pneumonitis. *Am J Pathol* 2011. **179**: 199-210.

51 **Avirutnan, P., Hauhart, R. E., Marovich, M. A., Garred, P., Atkinson, J. P. and Diamond, M. S.,** Complement-mediated neutralization of dengue virus requires mannose-binding lectin. *MBio* 2011. **2**.

52 **Avirutnan, P., Punyadee, N., Noisakran, S., Komoltri, C., Thiemmeca, S., Auethavornanan, K., Jairungsri, A., Kanlaya, R., Tangthawornchaikul, N., Puttikhunt, C., Pattanakitsakul, S. N., Yenchitsomanus, P. T., Mongkolsapaya, J., Kasinrerk, W., Sittisombut, N., Husmann, M., Blettner, M., Vasanawathana, S., Bhakdi, S. and Malasit, P.,** Vascular leakage in severe dengue virus infections: a potential role for the nonstructural viral protein NS1 and complement. *J Infect Dis* 2006. **193**: 1078-1088.

53 **Monsalvo, A. C., Batalle, J. P., Lopez, M. F., Krause, J. C., Klemenc, J., Hernandez, J. Z., Maskin, B., Bugna, J., Rubinstein, C., Aguilar, L., Dalurzo, L., Libster, R., Savy, V., Baumeister, E., Aguilar, L., Cabral, G., Font, J., Solari, L., Weller, K. P., Johnson, J., Echavarria, M., Edwards, K. M., Chappell, J. D., Crowe, J. E., Jr., Williams, J. V., Melendi, G. A. and Polack, F. P.,** Severe pandemic 2009 H1N1 influenza disease due to pathogenic immune complexes. *Nat Med* 2011. **17**: 195-199.

54 **Rodriguez-Madoz, J. R., Belicha-Villanueva, A., Bernal-Rubio, D., Ashour, J., Ayllon, J. and Fernandez-Sesma, A.,** Inhibition of the type I interferon response in human dendritic cells by dengue virus infection requires a catalytically active NS2B3 complex. *J Virol* 2010. **84**: 9760-9774.

55 **Garcia-Sastre, A., Egorov, A., Matassov, D., Brandt, S., Levy, D. E., Durbin, J. E., Palese, P. and Muster, T.,** Influenza A virus lacking the NS1 gene replicates in interferon-deficient systems. *Virology* 1998. **252**: 324-330.

56 **Arimori, Y., Nakamura, R., Yamada, H., Shibata, K., Maeda, N., Kase, T. and Yoshikai, Y.,** Type I interferon limits influenza virus-induced acute lung injury by regulation of excessive inflammation in mice. *Antiviral Research* 2013. **99**: 230-237.

57 **Price, G. E., Gaszewska-Mastarlarz, A. and Moskophidis, D.,** The role of alpha/beta and gamma interferons in development of immunity to influenza A virus in mice. *J Virol* 2000. **74**: 3996-4003.

58 **Szretter, K. J., Balish, A. L. and Katz, J. M.,** Influenza: propagation, quantification, and storage. *Curr Protoc Microbiol* 2006. **Chapter 15**: Unit 15G 11.

59 **Bruhl, H., Cihak, J., Plachy, J., Kunz-Schughart, L., Niedermeier, M., Denzel, A., Rodriguez Gomez, M., Talke, Y., Luckow, B., Stangassinger, M. and Mack, M.,** Targeting of Gr-1+,CCR2+ monocytes in collagen-induced arthritis. *Arthritis Rheum* 2007. **56**: 2975-2985.

Figure legends

Figure 1. Lethal disease during co-infection with influenza H1N1 and DENV. (A and B) Female *Ifnar*$^{-/-}$ mice were infected with H1N1 or DENV and, two days later, were co-infected with the other virus or inoculated with PBS for single-infected controls. (A) Graphs showing mean percent weight ±SEM over time of mice infected with H1N1 or DENV alone or co-infected with H1N1 followed two days later by DENV (H1N1–DENV) or DENV followed by H1N1 (DENV–H1N1). (B) Kaplan-Meier graphs showing percent survival of mice. (A and B) Data are pooled from three experiments (n=10-11 per group). * p<0.05; ** p<0.01; ***p<0.001; and ****p<0.0001 or non-significant (n.s.); (A) unpaired t-test or (B) the Log-rank (Mantel-Cox) test. For weight (A), significant differences between co-infection and infection with H1N1 alone are marked and were compared at the same time points after inoculation with H1N1.

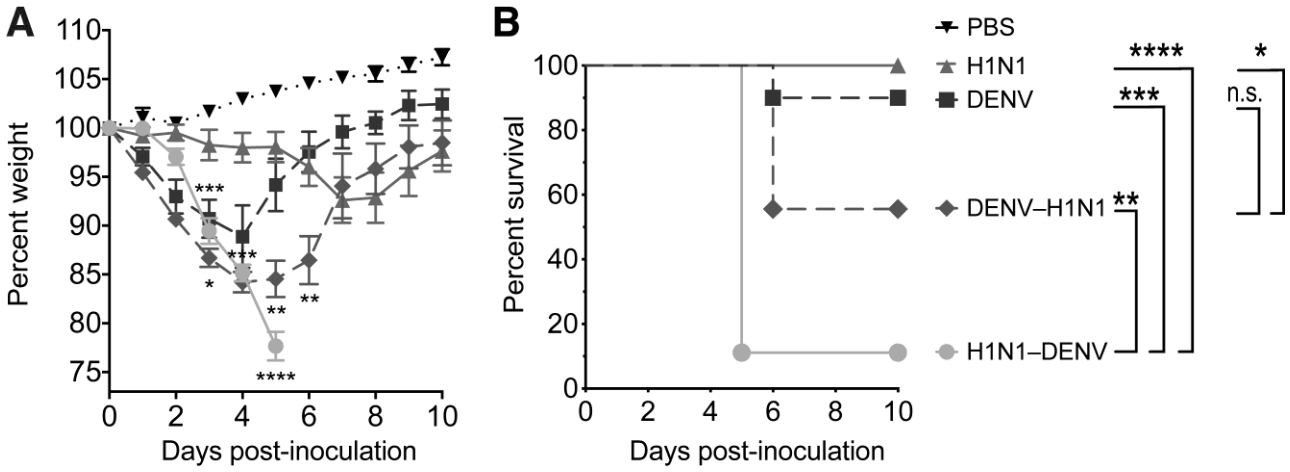

Figure 2. Increased DENV titers in mice with prior H1N1 infection. (A) H1N1 and (B) DENV titers in the lungs, and (B) livers or spleens of *Ifnar*$^{-/-}$ mice infected with H1N1 for 4 days and/or DENV for 2 days. (A and B) Graphs show single data points and median viral RNA genome equivalents normalized to µg mRNA of the *Gapdh* gene as measured by qRT-PCR in three experiments (n=9-11 per group). * p<0.05; unpaired Mann-Whitney test. The dotted horizontal lines mark the limit of detection.

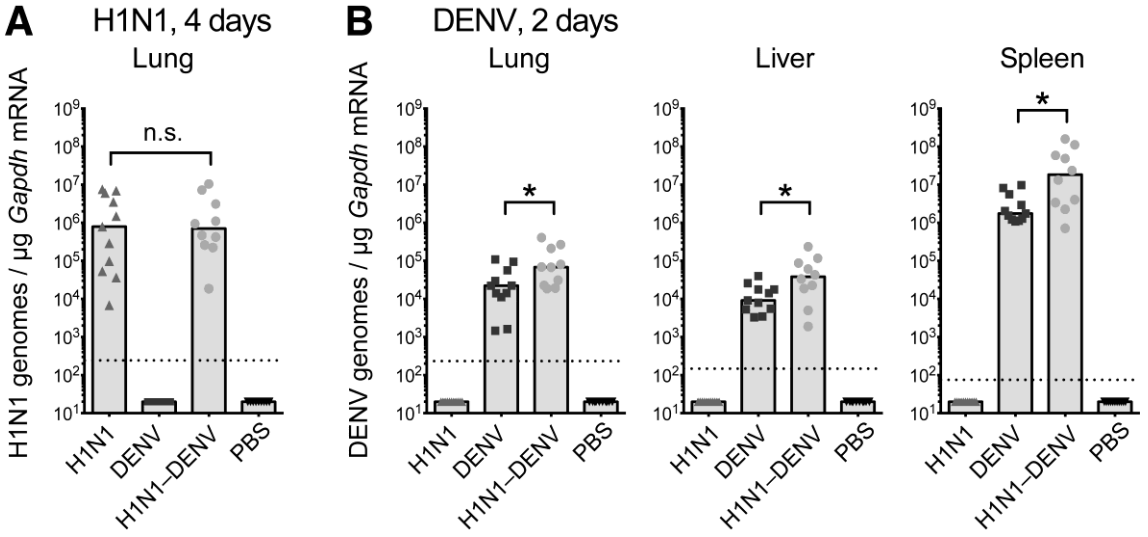

Figure 3. Histological analysis of spleens and livers of singly infected- and co-infected mice. (A) Histological sections stained with Hematoxylin and Eosin (H&E) of lungs from *Ifnar*$^{-/-}$ mice infected with H1N1 for 4 days and/or DENV for 2 days or inoculated with PBS. Black squares indicate enlarged areas. Solid arrows indicate areas of severe necrosis. (B)

Immunohistochemical staining of H1N1 antigen (brown) in lungs of the mice infected in (A). Dotted arrows indicate areas of H1N1-positive epithelial cells. Solid arrows indicate areas of necrosis. Data are representative for two experiments (*n*=6 per group).

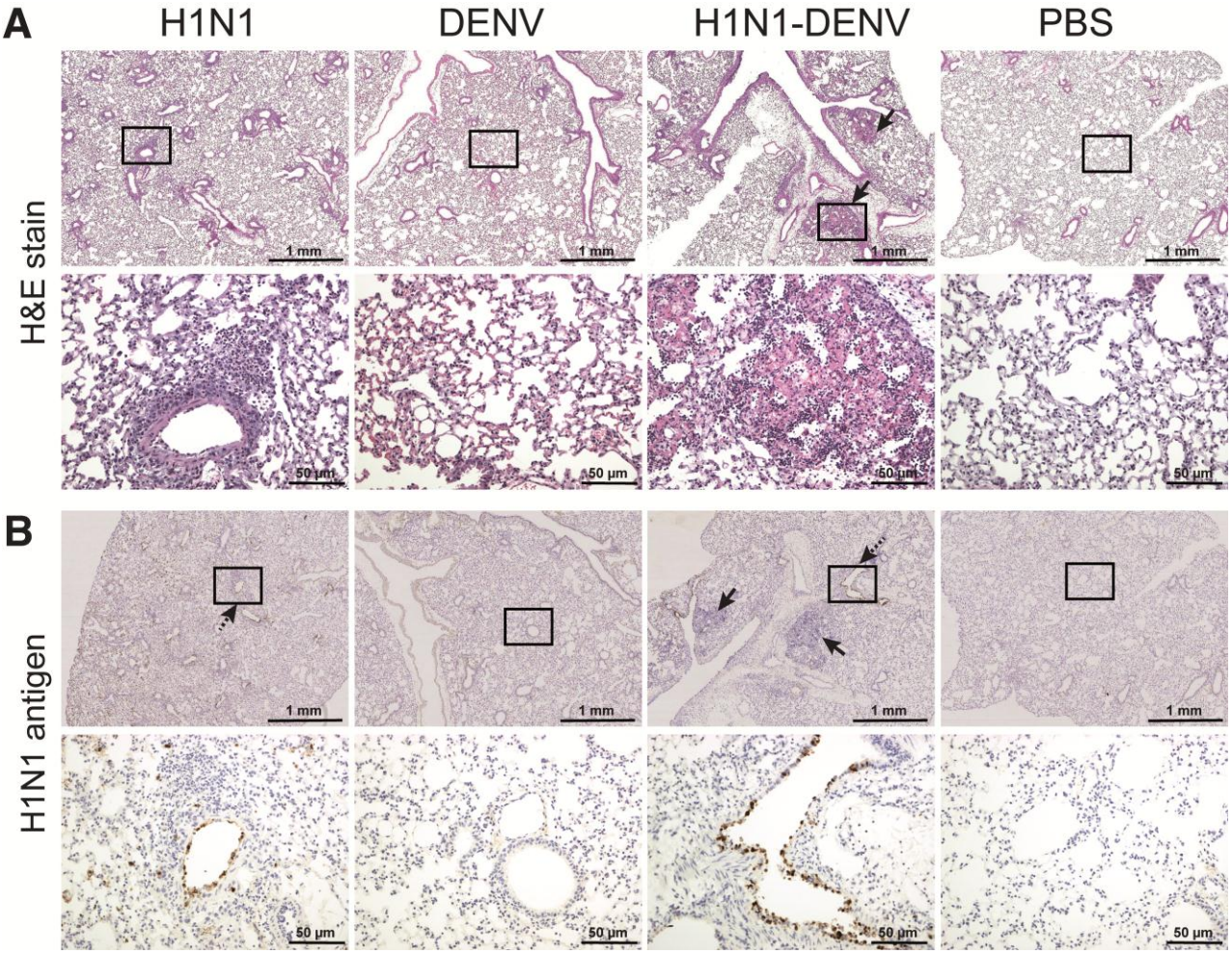

Figure 4. Partial mRNA responses against H1N1 or DENV infection in the lung. (A) Lungs of *Ifnar*$^{-/-}$ mice infected with H1N1 for 4 days and/or DENV for 2 days were analyzed for mRNA expression of 179 selected genes (nanoString). The Venn diagram shows that 29 genes were expressed significantly differently (unpaired t-test) between co-infection and single infection with H1N1 (but not single infection with DENV alone); 51 genes were expressed significantly differently between co-infection and single infection with DENV (but not single infection with H1N1 alone); and only 3 genes were expressed significantly differently between co-infection and single infection with either virus alone. (B-C) Clusters of genes for which co-infection induced significantly different mRNA expression compared to single infection with H1N1 (B) or DENV alone (C) that changed at least 2-fold compared to PBS controls and, when not correcting

for multiple comparisons, were significantly different from PBS controls. Genes marked in bold font and with a black asterisk were expressed significantly differently from PBS controls also after correcting for multiple comparisons (Holm-Sidak method). (D) Clusters of genes for which co-infection induced significantly different expression compared to single infection with H1N1 as well as single infection with DENV. (E) Heat map showing genes that were significantly changed during infection compared to PBS controls after correction for multiple comparisons. Tree showing unbiased clustering of samples (horizontal) or gene mRNA expression (vertical) after normalization via z-scoring by genes and samples (for labeling of genes see Suppl. Supporting information Fig. 4). Only one co-inoculated sample (i) and one sample inoculated with H1N1 alone (ii) did not cluster with the other samples from the same schedule of inoculation. (F) Gene families that during co-infection were expressed significantly differently from infection with H1N1 alone and followed a DENV signature (blue) are grouped on the left. Gene families that during co-infection were expressed significantly differently from infection with DENV alone and followed an H1N1 signature (red) are grouped on the right. Gene families that were shared between DENV and H1N1 signatures are illustrated in the center (black). Data were pooled from two experiments (n=6 per group).

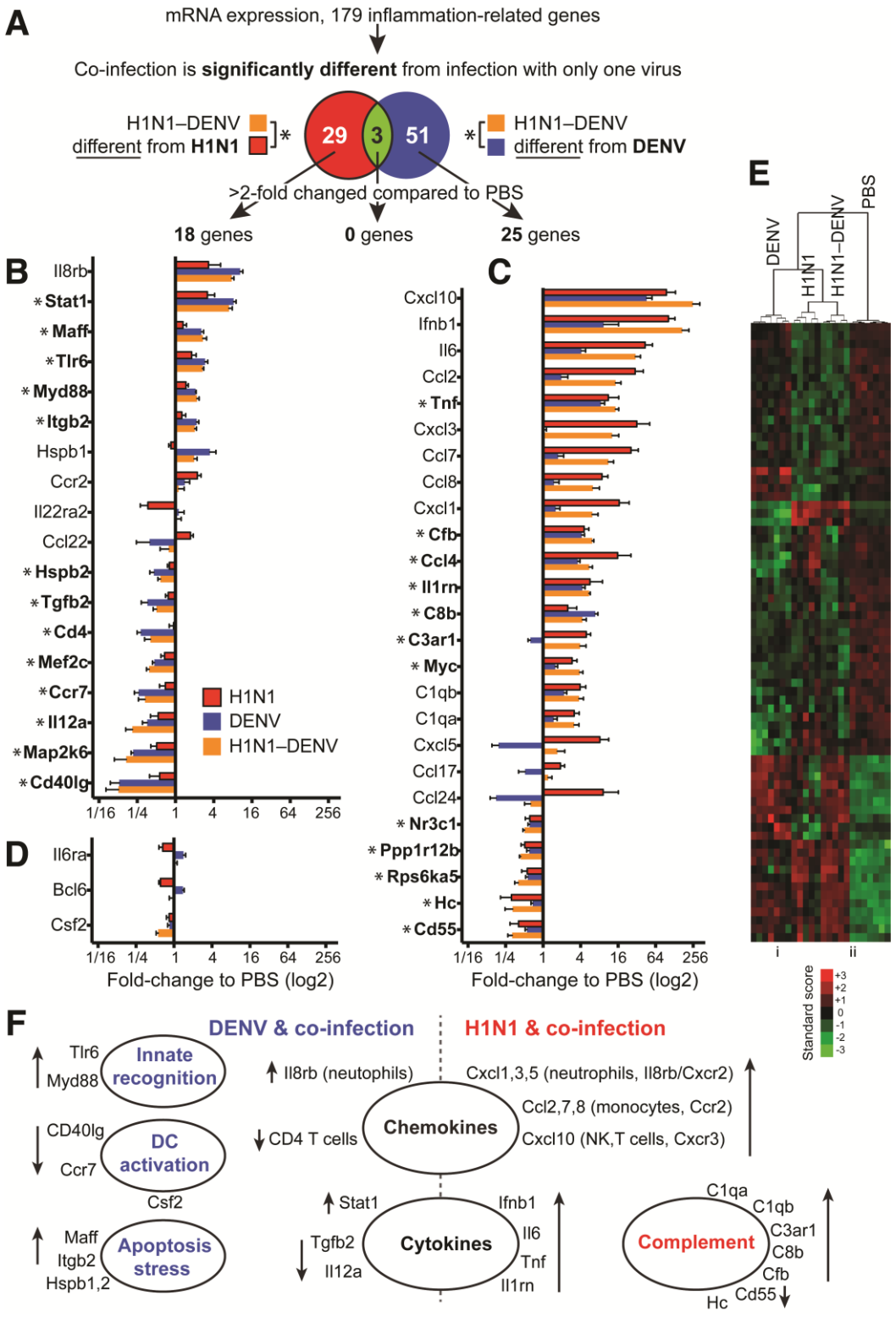

Figure 5. Impaired monocyte recruitment to co-infected lungs. (A) Contour plots showing CD45$^+$ cells in lungs of *Ifnar*$^{-/-}$ mice that were infected for 4 days with H1N1 and/or for 2 days with DENV and were analyzed via flow cytometry. Untreated mice served as steady-state controls. Consecutive gating identified CD11b^{high} Ly6G$^+$ neutrophils, Ly6G$^-$ CD11c$^+$ MHC II$^+$ DCs and macrophages, and Ly6G$^-$ CD11c$^-$ MHC II$^-$ CD11b$^+$ Ly6C$^+$ monocytes. (B and C) Bar graphs showing the mean ±SEM total number of (B) monocytes or (C) neutrophils in the lung, spleen, or bone marrow. Data are representative (A) or were pooled (B, C) from two experiments (n=6 per group). ** p<0.01; ***p<0.001; and ****p<0.0001 or non-significant (n.s.); one-way ANOVA (marked on top). If this test determined significant differences, one additional unpaired t-test determined whether significant differences existed between co-infection and infection with DENV alone (indicated below).

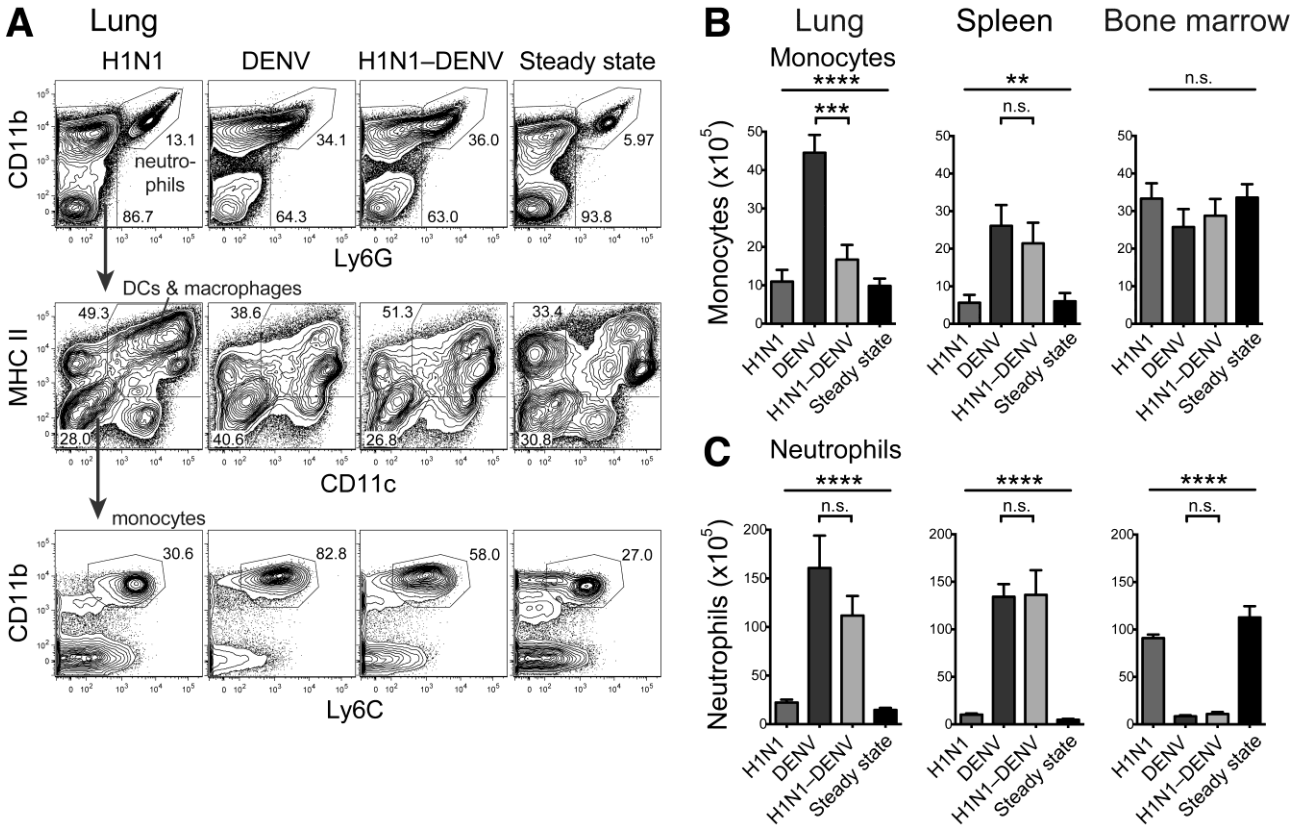

Figure 6. Monocyte numbers affect pathogenesis during co-infection. (A) Survival of co-infected *Ifnar*$^{-/-}$ mice that were adoptively transferred with monocytes 2 days after inoculation with H1N1 compared to controls not receiving transfer. Data were pooled from two experiments (n=6-9 per group). (B) Survival of co-infected mice that were depleted of monocytes via injection of anti-CCR2 antibody on days 1, 2, 3, and 4 after inoculation with H1N1 compared to

mice treated with isotype-matched control antibody. (A and B) Data were pooled from two experiments (n=6-9 (A) or n=6-7 (B) per group). * p<0.05; Log-rank (Mantel-Cox) test.

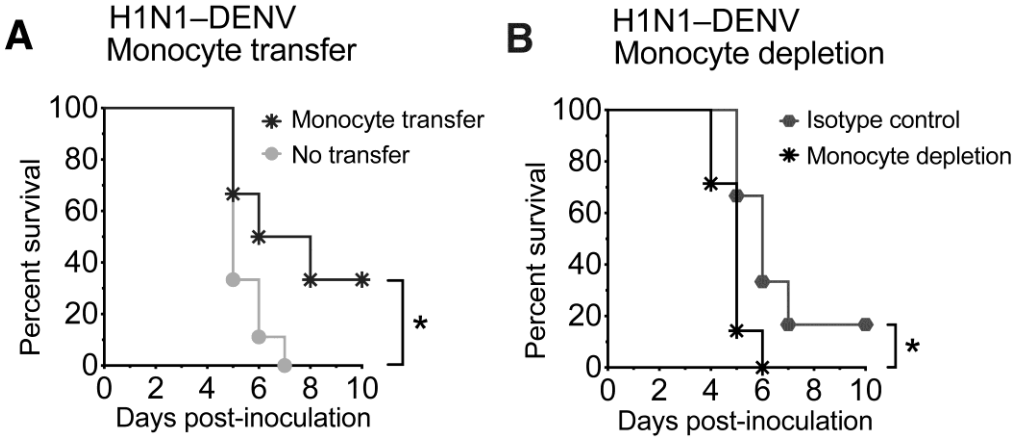

Graph Abstract